Universality of the perturbative definition of the Flory-Huggins parameter

Artem Petrov [1,*] Guillermo A. Hernández-Mendoza [2] and Alfredo Alexander-Katz [2,†]
[1]*Department of Chemical Engineering, Massachusetts Institute of Technology, Cambridge, Massachusetts 02139, USA*
[2]*Department of Materials Science and Engineering, Massachusetts Institute of Technology, Cambridge, Massachusetts 02139, USA*

(Received 28 July 2025; accepted 19 February 2026; published 9 March 2026)

The effective Flory-Huggins parameter χ_e is one of the most important characteristics of any multicomponent polymer system. This parameter characterizes the free energy of interaction between monomers of different types and controls the phase behavior of polymer mixtures. In this work, we developed a perturbation theory and derived how χ_e depends on the details of an arbitrary coarse-grained polymer model. After defining χ_e in this way, we found that the models of symmetric polymer blends and diblock copolymer melts behaved universally: Their phase transition points, free energies, and mesoscopic invariant structure factors depended solely on the chain architecture, the invariant chain length $\bar{N}$, and the interaction parameter $\chi_e N$. To parametrize our perturbative expression for χ_e, only the effective coordination number distribution in a reference homogeneous system needs to be measured. This distribution, in turn, can be directly mapped onto coarse-grained model parameters set prior to simulation, which clarifies how model construction influences χ_e. Our definition of χ_e enables straightforward quantitative comparison of models with each other and with experiments, which will facilitate the computational design of multicomponent polymer materials.

DOI: 10.1103/532b-lhkh

I. INTRODUCTION

Multicomponent polymer materials, which include blends and block copolymers, are widely used in industry and nanotechnology [1,2]. Nevertheless, discovering and predicting morphologies and properties of such materials remain a major challenge [3]. Especially for complex materials and systems with long chains, coarse-grained computer modeling is much preferred over atomistic simulations for such discovery [4–6]. However, it is very hard to relate the parameters of an arbitrary coarse-grained model (a "model" stands for a set of system parameters and interaction potentials in a simulation) to the experimental quantities such as temperature T, pressure, pH, etc. This, in turn, limits the ability of coarse-grained modeling to provide quantitative experimental predictions, which hampers the development of materials.

This model-experiment correspondence can be constructed using the so-called universality hypothesis [7,8], which states that the key properties of polymer materials should depend only on a handful of effective quantities [9–12]. In the special case of structurally symmetric two-component systems, their universal behavior implies that their free energy and the mesoscopic structure depend only on three factors: (1) chain architecture, (2) the invariant chain length $\bar{N}$, which is roughly equal to the squared average number of chains fitting in a volume spanned by a chain in a melt [7], and (3) the interaction parameter $\chi_e N$, where N is the number of monomers in a chain and χ_e is the effective Flory-Huggins parameter. χ_e characterizes the strength of interaction between different species and is defined in Eq. (1) (for simplicity, we will consider only two-component systems in this work) [13].

$$\chi_e \equiv -\frac{1}{2k_B T}\frac{\partial^2 \Delta f_{\text{int}}}{\partial \phi^2}. \tag{1}$$

In Eq. (1), Δf_{int} is the interaction free energy of mixing per monomer, which can be determined as the $N \to \infty$ limit of the true free energy of mixing [13]. $\phi \equiv \phi_A$ is the volume fraction of the A-type monomers [since blends and diblock copolymer (DBC) melts are typically considered incompressible, $\phi_B = 1 - \phi$].

The universality hypothesis implies that one can experimentally reproduce a certain phase discovered in a coarse-grained simulation if the experimental system and the model have matching effective parameters, including the chain architecture, $\bar{N}$, and $\chi_e N$ [14,15]. Except for $\chi_e N$, it is possible to match all of these effective quantities in simulations to the experimental systems relatively straightforwardly [14].

On the other hand, χ_e is a difficult quantity to estimate both in simulations and experiments. One way to define the experimental $\chi_e(T)$ function is to use the universality hypothesis again and to relate the phase transition temperatures to the universal prediction of $\chi_e N$ at the transition point obtained from simulations [7,16,17]. Therefore, to build the model-experiment correspondence (as well as to construct a mapping between the parameters of different coarse-grained models), one needs to define χ_e in such a way that all models behave universally. However, to the best of our knowledge, an

*Contact author: aipetrov@mit.edu
†Contact author: aalexand@mit.edu

Published by the American Physical Society under the terms of the Creative Commons Attribution 4.0 International license. Further distribution of this work must maintain attribution to the author(s) and the published article's title, journal citation, and DOI.

analytical expression for χ_e as a function of coarse-grained model parameters that has this property was not obtained before.

Previously, an attempt to solve this challenge was made by Morse and co-workers [7,8,18]. These authors recognized that χ_e should be defined as a function of α, where $\alpha \equiv a_{AB} - (a_{AA} + a_{BB})/2$ is the microscopic parameter controlling the segregation between species. The energy parameters a_{ij} control the nonbonded pairwise interaction potential in a coarse-grained model, which in general can be written as $w_{ij} = a_{ij} v(r_{ij})$, where $v(r_{ij})$ is a dimensionless function of the distance between monomers i and j, and a_{ij} depend on the type of the monomers (A or B) [7,13,16,19–22] (typically, $a_{AA} = a_{BB} \equiv a_{xx}$). Morse *et al.* did not derive the expression for the $\chi_e(\alpha)$ function or its coefficients. Instead, they suggested that in the limit of infinitely small $A - B$ segregation ($\alpha \to 0$), $\chi_e(\alpha)$ should scale linearly with α as originally proposed by Flory. In particular, Morse and Chung [13] used first-order perturbation theory to derive the expression $\chi_e(\alpha \to 0) \to z_\infty \alpha / k_B T$, where z_∞ is the effective coordination number of a given model with infinitely long chains measured at $\alpha = 0$. Since it was shown that this first-order perturbative expression for $\chi_e(\alpha)$ yields the universality of only a class of coarse-grained models [16], nonlinear terms have to be added. Chung [18] attempted to build a second-order perturbative expression for $\chi_e(\alpha)$ analytically; however, the coefficients in that expression could not be estimated with adequate precision from simulations, and unknown two-loop corrections further hampered the calculation of χ_e up to the second order in α. Other works added several nonlinear terms with undefined coefficients somewhat arbitrarily [22], and the expression for $\chi_e(\alpha)$ became either a polynomial or a ratio of polynomials [7,21–23]. The coefficients for the nonlinear terms were defined by fitting the peak scattering intensity measured at various α and N in a given model to the predictions of the renormalized one-loop (ROL) theory. Such nonlinear expressions for $\chi_e(\alpha)$ yielded the universal behavior of all studied coarse-grained models [7]; however, this fitting-based approach has several downsides. First, the fitting procedure itself is difficult and computationally intensive, since it requires the calculation of complex ROL Fourier integrals and the simulation of a model at several different values of N and α; harder-to-equilibrate systems close to phase transition also need to be simulated. Second, the nature of nonlinear corrections to χ_e (and, therefore, to Δf_{int}) remains obscure, which limits the understanding of how the model's free energy depends on its microscopic parameters. Third, the correctness of the ROL theory predictions for peak scattering intensity (including the universality of this quantity) is assumed during this procedure at least for one chain length [22]. Although this theory has validation independent of the definition of χ_e (and the mere existence of an N-independent $\chi_e(\alpha)$ function that is able to fit ROL predictions provides some support to the theory [22]), some simulation data demonstrate significant deviations from the theoretical predictions [22]. Since the ROL theory effectively gives the expression for (a group of) $\chi_e(\alpha)$ functions via the fitting procedure, the development of a separate first-principles analytical theory for $\chi_e(\alpha)$ can provide additional test to the ROL approach and the universality hypothesis in general.

In this work, we developed a generalization of the first-order perturbation theory by Morse and Chung [13]. Using our theory, we obtained an analytical expression for χ_e as a series in powers of $\alpha / k_B T$. The coefficients of this expansion are fully defined by the cumulants of the distribution of a single microscopic model-specific quantity—effective coordination number z. These cumulants have to be measured only in the homogeneous reference state (i.e., at $\alpha = 0$), which makes the estimation of χ_e for a given model much more straightforward and computationally efficient than previously developed approaches [7,8,21–23]. Using molecular dynamics simulations and the available data on lattice models and field-theoretic simulations (FTSs), we showed that this definition of χ_e produces universal behavior of all studied models. Moreover, we derived a separate theory and obtained the cumulants of z as functions of coarse-grained model parameters set prior to simulation. This mapping revealed that the parameters mostly influencing the value of χ_e in continuum particle-based models are a_{xx} and the monomer number density ρ. Moreover, the theory successfully predicted that a_{xx} defines the convergence radius of the $\chi_e(\alpha)$ series and χ_e can be represented as a polynomial in powers of $\alpha / k_B T$, whose order is defined mostly by the product of ρ and chain length N at a fixed value of $\chi_e N$. As a result, we obtained an analytical expression for χ_e, which led to the universal behavior of models and has clear dependence on the parameters of an arbitrary coarse-grained model of a multicomponent polymer system. This expression clarified the physical nature of χ_e in coarse-grained models and confirmed the existence of universality of finite-length polymer systems without assuming the universality of any of the model characteristics. Our approach will significantly simplify the quantitative prediction of experiments with coarse-grained simulations, which can facilitate development of polymer materials using computational tools.

II. PERTURBATION THEORY: χ_e AS A FUNCTION OF COARSE-GRAINED MODEL PARAMETERS

To obtain an analytical expression for χ_e as a function of α and other coarse-grained model parameters, we developed an approach to performing the cumulant expansion of the free energy of a disordered binary polymer blend. Despite the fact that this derivation was performed for blends, it is applicable to models of other multicomponent polymer systems, for instance, block copolymer melts, since χ_e is a local parameter that does not depend on the chain architecture [13]. In this section, we will outline the key steps in the derivation; see Sec. 1 in the Supplemental Material [24] for more details .

The expression for $\chi_e(\alpha)$ is derived for coarse-grained models, which can be described by nonbonded pairwise interaction potential $w_{ij} = a_{ij} v(r_{ij})$; we will assume that $a_{AA} = a_{BB} \equiv a_{xx}$ (therefore, $\alpha = a_{AB} - a_{xx}$ in this work). As a result, the total potential energy $U[\mathbf{R}]$ of the system in a given configuration $\mathbf{R}$ can be written as

$$U[\mathbf{R}] = U_b[\mathbf{R}] + \frac{1}{2} a_{xx} \sum_{k=1}^{N_t} \sum_{i=1, i\neq k}^{N_t} v_{ik} + \alpha \sum_{\gamma \in C} v_\gamma . \quad (2)$$

In Eq. (2), $U_b[\mathbf{R}]$ is the potential energy of bonded interactions in the given configuration, N_t is the total number of

monomers in the system, and C is a set of unique monomer pairs (i, k) that have different types: $C = \{(i, k) : \text{type}(i) = A, \text{type}(k) = B\}$; index γ enumerates such pairs. The first two summands in Eq. (2) represent the total potential energy in a fully homogeneous blend (at $\alpha = 0$). Upon inserting Eq. (2) into the expression for the free energy per monomer and by invoking the definition of χ_e [Eq. (1)], we can obtain the following general perturbative formula for χ_e:

$$\chi_e(\alpha, \phi) = \frac{1}{2N_t}\frac{\partial^2}{\partial\phi^2}\left(\sum_{n=1}^{\infty}\frac{(-1)^n}{n!}\left(\frac{\alpha}{k_BT}\right)^n \kappa_n\left[\sum_{\gamma\in C} v_\gamma\right]_{0,\text{int}}\right). \tag{3}$$

In Eq. (3), $\kappa_n[\sum_{\gamma\in C} v_\gamma]_{0,\text{int}}$ are the N-independent coefficients characterizing the perturbative expansion of Δf_{int}, which are given by the following expression:

$$\kappa_n\left[\sum_{\gamma\in C} v_\gamma\right]_{0,\text{int}} \equiv \kappa_n\left[\sum_{\gamma\in C} v_\gamma\right]_0 - \frac{N_t}{N}(-1)^{n+1} \times \left.\frac{\partial^n f^*}{\partial(\alpha/k_BT)^n}\right|_{\alpha=0}. \tag{4}$$

In Eq. (4), f^* denotes the finite-N correction to the excess free energy per monomer f_{ex} of a blend; f^* tends to zero as chains become infinitely long [18]. $\kappa_n[\sum_{\gamma\in C} v_\gamma]_0$ is the nth cumulant of the distribution of dimensionless total potential energy of nonbonded interaction of opposite-type monomers. These cumulants characterize the perturbative expansion of f_{ex} and are measured in the reference state (fully homogeneous polymer blend, $\alpha = 0$). Further, we will focus on the calculation of $\kappa_n[\sum_{\gamma\in C} v_\gamma]_0$. By analyzing the N-dependence of $\kappa_n[\sum_{\gamma\in C} v_\gamma]_0$, we will extract the required $\kappa_n[\sum_{\gamma\in C} v_\gamma]_{0,\text{int}}$ coefficients as functions of ϕ and coarse-grained model parameters. Equation (3) is an example of the classic cumulant expansion of the free energy applied to binary polymer blends.

Despite the seeming simplicity of Eq. (3), the cumulants of the total potential energy distribution are nearly impossible to estimate accurately due to the necessity of extensive whole-system sampling [25]. Instead, due to the multilinearity of cumulants [26], we can express $\kappa_n[\sum_i x_i]$ as a multisum over joint cumulants $\kappa[x_1, ..., x_n]$:

$$\kappa_n\left[\sum_{\gamma\in C} v_\gamma\right]_0 = \sum_{\gamma_1,\ldots,\gamma_n} \kappa\left[v_{\gamma_1}, \ldots, v_{\gamma_n}\right]_0. \tag{5}$$

In this multisum, indices $\gamma_1, \ldots, \gamma_n$ denote distinct unique pairs of opposite-type monomers. If one retains all these joint cumulants in the final expression for χ_e, the measurement of a prohibitively large number of statistical quantities in the reference state will be needed in order to parametrize the expression. Moreover, ϕ and N dependencies of arbitrary joint cumulants are generally unknown, which will preclude one from calculating χ_e using Eq. (3) for a given coarse-grained model even after measuring various joint cumulants at a certain N and ϕ.

Therefore, we decided to simplify Eq. (5) by making assumptions about the dominant microscopic correlations in the reference polymer blend model. We can hope that these simplifications will allow us (1) to retain the dominant fluctuations crucial for determining χ_e accurately and (2) to approximate $\kappa_n[\sum_{\gamma\in C} v_\gamma]_0$ up to arbitrary n by quantities that are simply calculable and that have known ϕ and N dependencies. This, in turn, will make possible the extraction of N-independent $\kappa_n[\sum_{\gamma\in C} v_\gamma]_{0,\text{int}}$ cumulants as functions of ϕ and allow differentiation with respect to ϕ as required by Eq. (3) in order to obtain $\chi_e(\alpha)$ for a given model.

We can subdivide the joint cumulants in Eq. (5) into three categories. The first category features cumulants in which all γ_j's are equal (only one monomer pair determines a given joint cumulant). The second category includes the cumulants involving three different monomers (more precisely, those cumulants are included in the second category in which $\gamma_1 = \cdots = \gamma_r \neq \gamma_{r+1} = \cdots = \gamma_n$, the first r γ indices can be distributed in any order among n indices, r can be any number between 1 and $n-1$, and one monomer index is the same in both pairs γ_r and γ_{r+1}). Finally, the third category contains cumulants involving four and more monomers. In this work, we consider joint cumulants belonging to the third category equal to zero; this approximation is equivalent to assuming that in any set of four and more monomers, there will be a subset of pairs in which monomer-monomer distances are independent of the distances in the other subset [26]. In other words, we neglect the "true," collective correlations between positions of four and more particles in the homogeneous blend. This assumption can be justified by the short-range nature of the monomer-monomer interaction potential w_{ij}. Three-monomer cumulants can be nonzero, however, since they describe the correlations between two monomers interacting with each other and situated in the vicinity of a common third monomer, and these correlations can be nontrivial.

In such a simple perturbative model of a polymer blend, Eq. (5) becomes

$$\kappa_n\left[\sum_{\gamma\in C} v_\gamma\right]_0 \approx \phi(1-\phi)N_t^2\kappa_n[v]_0 + \frac{1}{2}\phi(1-\phi)N_t^3 \times \sum_{r=1}^{n-1}\binom{n}{r}\kappa(r, n)_0. \tag{6}$$

In Eq. (6), $\kappa_n[v]_0$ and $\kappa(r, n)_0$ denote $\kappa_n[v_\gamma]_0$ and $\kappa[\underbrace{v_\gamma, \ldots, v_\gamma}_{r\text{ times}}, \underbrace{v_\delta, \ldots, v_\delta}_{n-r\text{ times}}]_0$, respectively, for any γ and δ. Section 1 in the Supplemental Material [24] contains the full details of the derivation of Eq. (6); during this derivation, we additionally assumed the weakness of collective correlations between three monomers, two of which are situated on the same chain (since there is much fewer such triplets of monomers compared to the triplets in which all monomers are located on different chains).

As a final derivation step, we can express Eq. (6) as an nth cumulant of the effective coordination number z. For a given monomer k in a given system configuration, we can define z_k as a sum of v_{ik} values such that monomers i and k are located on different chains:

$$z_k \equiv \sum_{i:\text{chain}(i)\neq\text{chain}(k)} v_{ik}, \tag{7}$$

where z_k is a configuration-dependent random variable; its nth cumulant can be calculated similarly to Eq. (6) by invoking the approximation of vanishing joint cumulants of v_{ik} if they

involve four or more monomers and if they involve three monomers, two of which lie on the same chain:

$$\kappa_n[z_k]_0 = \kappa_n[z]_0 \approx N_t \kappa_n[v]_0 + \frac{1}{2} N_t^2 \sum_{r=1}^{n-1} \binom{n}{r} \kappa(r, n)_0. \quad (8)$$

Comparing Eqs. (6) and (8), we can arrive at the following approximation: $\kappa_n[\sum_{\gamma \in C} v_\gamma]_0 \approx \phi(1-\phi) N_t \kappa_n[z]_0$. The distribution of the model-dependent microscopic property z is ϕ independent and can be easily sampled. Moreover, as shown in Sec. 2 in the Supplemental Material [24], the ROL theory [13] demonstrates that $\kappa_n[z]_0$ is expected to have the following N dependence: $\kappa_n[z]_0 \approx \kappa_n[z]_{0,N\to\infty} + C/N^{1/2}$, where C is a model-dependent constant. Therefore, the N-independent part of $\kappa_n[\sum_{\gamma \in C} v_\gamma]_0$ equals to $\phi(1-\phi) N_t \kappa_n[z]_{0,N\to\infty}$. If we neglect weak two- and higher-loop contributions to f^*, $\partial^n f^*/\partial \alpha^n|_{\alpha=0}$ derivatives will have N dependence of the type $\sum_i a_i N^{x_i}$, where a_i and x_i are nonzero constants [18]. Therefore, $\phi(1-\phi) N_t \kappa_n[z]_{0,N\to\infty}$ will be the only N-independent term on the right-hand side of Eq. (4). As a result, the N-independent quantity $\kappa_n[\sum_{\gamma \in C} v_\gamma]_{0,\text{int}}$ will be equal to $\kappa_n[\sum_{\gamma \in C} v_\gamma]_{0,\text{int}} = \phi(1-\phi) N_t \kappa_n[z]_{0,N\to\infty}$ in our approximate perturbation theory. The accuracy of this approximation is confirmed by evaluating the contribution of excluded multimonomer correlations to χ_e in Sec. 7 in the Supplemental Material [24]. As a result, the perturbation theory outlined above led to a calculable expression for $\kappa_n[\sum_{\gamma \in C} v_\gamma]_{0,\text{int}}$ with known ϕ dependency for all n. Thus, we can insert this formula into Eq. (3) and arrive at the final perturbative expression for χ_e:

$$\chi_e(\alpha) = \sum_{n=1}^{\infty} \frac{(-1)^{n+1}}{n!} \left(\frac{\alpha}{k_B T} \right)^n \kappa_n[z]_{0,N\to\infty}. \quad (9)$$

Equation (9) represents the key result of the perturbation theory presented in this work. Equation (9) has a clear physical meaning: The corrections to the linear Flory-like result $\chi_e \propto \alpha$ stem from the fluctuations of the effective coordination number in the fully homogeneous state of multicomponent polymer systems. Furthermore, to calculate $\chi_e(\alpha)$ up to an arbitrary order n for a given model, one needs to measure the n first cumulants of only a single microscopic random variable z at $\alpha = 0$ and extrapolate them to $N \to \infty$ using the analytical expression above (see also Sec. 2 in the Supplemental Material [24]). Therefore, no additional simulations and theoretical calculations at $\alpha \neq 0$ are required to parametrize the expression for $\chi_e(\alpha)$. This provides a significant computational advantage compared to the previous fitting-based methods of $\chi_e(\alpha)$ estimation [7,8,21–23], which required complex calculations and model simulation at $\alpha > 0$.

It is worth mentioning that truncating Eq. (9) at $n = 1$ yields the exact first-order perturbative result [13], since $\kappa_1[z]_{0,N\to\infty} = \langle z_i \rangle_{0,N\to\infty} \equiv z_\infty$, where z_∞ is the average effective coordination number evaluated in the reference homogeneous system with infinite chains defined in Refs. [13,22]. Moreover, in Eq. (9), χ_e does not depend on ϕ; this is an artifact of neglecting joint cumulants involving four and more monomers during the evaluation of $\kappa_n[\sum_\gamma v_\gamma]_0$. However, simulation data in Sec. 7 in the Supplemental Material [24] suggest that the inclusion of these cumulants will likely have a minor effect on $\chi_e(\alpha)$; moreover, previous research [27,28] showed that neglecting the ϕ dependence of the fitting-based ROL-theoretic χ_e does not influence its ability to yield the universality of models at all ϕ.

Importantly, the analyticity and simplicity of Eq. (9) allow an explicit qualitative description of how model parameters influence χ_e. This can be done by developing a separate simple theory describing the distribution of the effective coordination number z in the reference system (i.e., at $\alpha = 0$ and $N \to \infty$). In this work, we will focus on the continuum particle-based models (see Sec. 8 in the Supplemental Material [24] full derivation); however, the theory can be readily built for lattice models and field-theoretic simulations as qualitatively done in Section 4 in the Supplemental Material [24]. In short, we assume that (1) each monomer in a model has a defined number of other-chain neighboring monomers k within the interaction range, (2) the distances between the neighbors and the selected monomer are independent of each other, and (3) monomer density ρ is small and $a_{xx}/k_B T$ is large. These assumptions allowed to write a simple probability distribution of monomer-monomer distances r_{ij} and allowed inversion of the $v(r_{ij})$ function. As a result, the random variable z defined in Eq. (7) was derived to be distributed according to the gamma distribution with the shape parameter $\alpha = k/2$ [for all $v(r)$ having a minimum at the cutoff distance] and the scale parameter $\theta = k_B T/a_{xx}$. Moreover, low ρ and high $a_{xx}/k_B T$ are typically achieved in models with "soft" enough repulsive nonbonded interactions; in such models, k depends weakly on all model parameters except for ρ ($k \approx 4\rho$; see Fig. S9 in Ref. [16]). Therefore, $\kappa_n[z]_{0,N\to\infty}$ in this approximation will be equal to

$$\kappa_n[z]_{0,N\to\infty} \approx 2\rho(n-1)!(k_B T/a_{xx})^n. \quad (10)$$

As a result, the model-dependent coefficients in the expression for $\chi_e(\alpha)$ [Eq. (9)] are predicted to be determined solely by the values of ρ/a_{xx}^n at a fixed T. Moreover, inserting Eq. (10) into Eq. (9) leads to the estimation of the convergence radius of Eq. (9). In this simple theory, Eq. (9) will converge for all $\alpha < a_{xx}$. Finally, Eq. (10) allowed us to analyze the partial sums of the series in Eq. (9). By dividing the leading terms of the remainder and of the nth partial sum of Eq. (9) using Eq. (10), we predicted the smallest order n at which the series in Eq. (9) can be truncated in order to produce accurate enough estimation of χ_e. At a fixed $\chi_e N$, this order was found to depend only on the product $N\rho$ (see Sec. 8 in the Supplemental Material [24] for a more detailed derivation). Bigger $N\rho$ reduced the order of truncation; in turn, this predicted the existence of finite-N models for which the linear $\chi_e \propto \alpha$ approximation works accurately at or below the order-disorder transition (ODT) point, which explains our recent findings [16]. Such correspondence between the model parameters and χ_e was not available in previous fitting-based approaches [7,8,21–23].

The established dependence of $\chi_e(\alpha)$ truncation order on the model parameters can be qualitatively explained as follows. At all model parameters fixed, an increase of $\chi_e N$ implies the increase of the value of α closer to the convergence radius $\approx a_{xx}$. This, in turn, increases the order up to which Eq. (9) should be truncated to be accurate up to the increased $\chi_e N$. In addition, increasing N reduces the value of χ_e and,

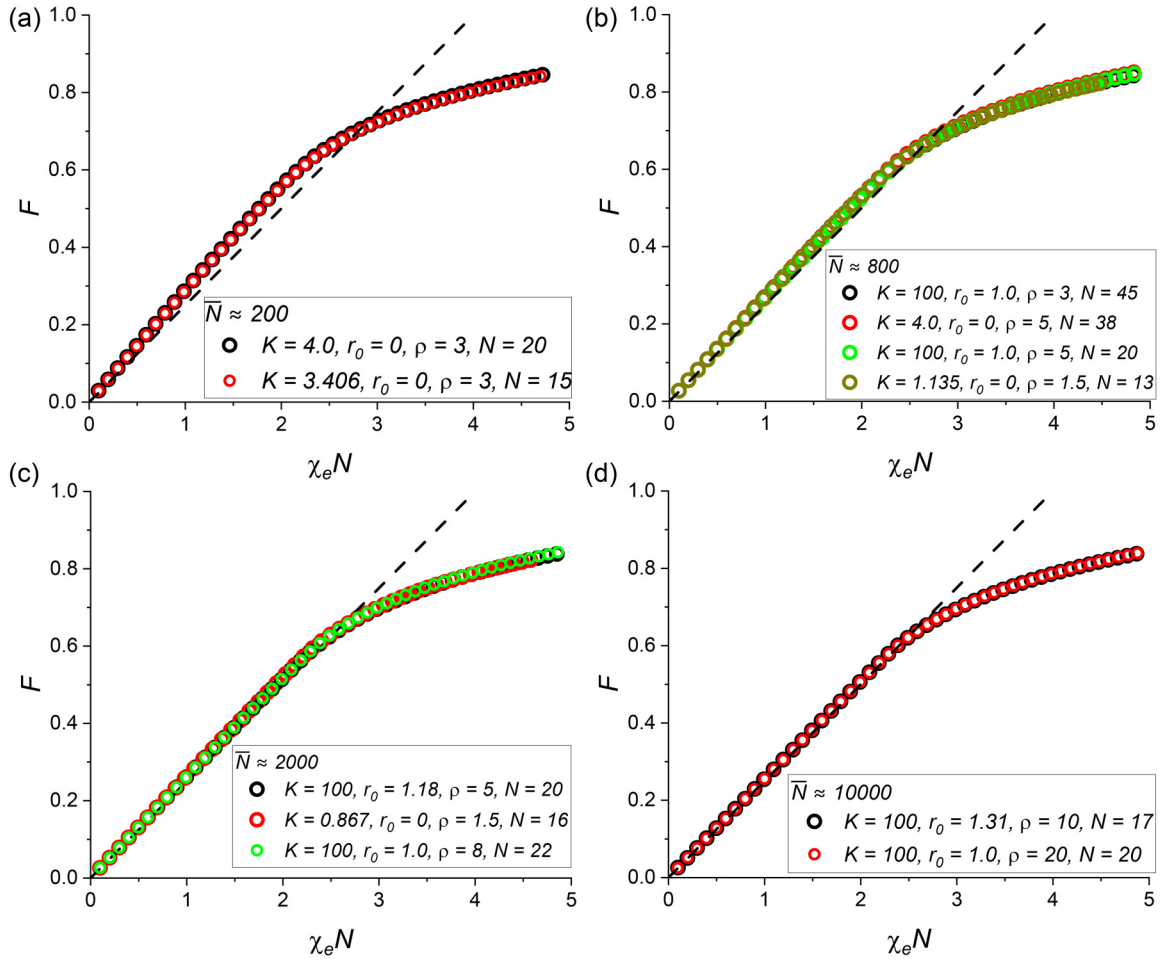


FIG. 1. $\chi_e N$ dependencies of the excess free energy per chain F for different models of symmetric binary blends with soft repulsive potential. Each panel contains plots for models having similar $\bar{N}$; points of different colors correspond to different models. Except for models with $\rho = 1.5$, a_{xx} was calculated as $a_{xx} = 75/\rho$ to mimic the compressibility of water [30]. Models with $\rho = 1.5$ had $a_{xx} = 25$ as in Ref. [7]. Dashed lines show the mean-field prediction $F = \chi_e N/4$.

therefore, α, necessary to achieve a given $\chi_e N$ (when $\chi_e N$ and all other model parameters are fixed). As a result, increasing N leads to a smaller polynomial order of $\chi_e(\alpha)$. Finally, an increase of ρ leads to a decrease of this order (when $\chi_e N$ and all other model parameters are fixed). This occurs due to a coincidence of two factors: (1) higher ρ leads to a higher average z, which reduces the value of α necessary to reach the given $\chi_e N$, and (2) $\kappa_2[z]_{0,N\to\infty}$ scales weaker than ρ^2 [Eq. (10)]. Importantly, Eq. (10) predicted that other model parameters affect the truncation order weakly.

III. SIMULATION METHODS

To test the predictions outlined above and to check whether the perturbative definition of $\chi_e(\alpha)$ in Eq. (9) can yield the universality of coarse-grained models of multicomponent polymer systems, we performed molecular dynamics (MD) simulations of symmetric binary blends and symmetric diblock copolymer melts. In MD, a bead-and-spring model was used to represent coarse-grained polymers. Temperature was fixed to $k_B T = 1$ and bonds were modeled with harmonic potential $U_b = K(r_{ij} - r_0)^2/2$, where K and r_0 are the bond strength and rest length, respectively. For models with soft repulsive potentials, the nonbonded interactions were modeled with $v(r_{ij}) = 0.5(1 - r_{ij})^2$ for $r_{ij} < 1$ and $v(r_{ij}) = 0$ otherwise. We also studied one model (denoted as H model) with harsh repulsion between monomers modeled by a Lennard-Jones potential: $v(r_{ij}) = 4[(1/r_{ij})^{12} - (1/r_{ij})^6 + 1/4]$ for $r_{ij} < 1.1225$ and $v(r_{ij}) = 0$ otherwise. To make our models structurally symmetric, we set the same bond parameters for both A and B monomer species, same-type repulsion parameters to $a_{AA} = a_{BB} \equiv a_{xx}$, and the fraction of A-type monomers to $f = N_A/N_t = 0.5$. As mentioned in the introduction, we refer to a "model" as a choice of the form of repulsive potential and the set of the following parameters: a_{xx}, K, r_0, N, and ρ. According to our definition of a "model," these quantities are fixed and independent of the control parameter α, which was tuned by varying a_{AB} (see Sec. 6 in the Supplemental Material [24] for discussion of other possible definitions). The model parameters will determine $\kappa_n[z]_{0,N\to\infty}$ and $\bar{N}$; the latter equals to $\bar{N} = N\rho^2 b^6$, where b is the statistical segment length; b^2 is defined as the $N \to \infty$ limit of $6R_g^2/N$, where R_g is the chain radius of gyration (SM Sec. 2 in the Supplemental Material [24]). a_{AB} is not considered a model parameter, since it does not affect other quantities except for α. Truncation of Eq. (9)

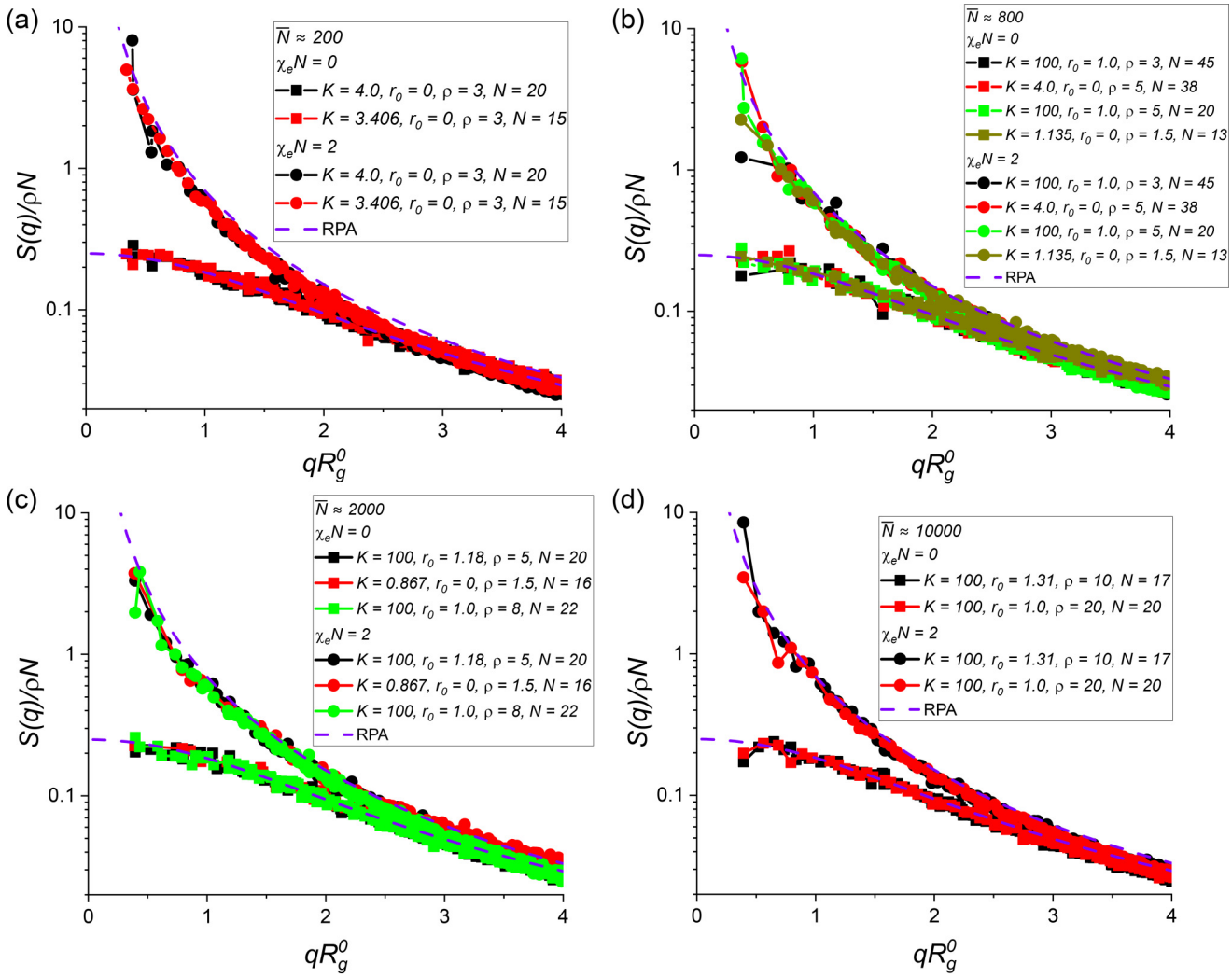


FIG. 2. The invariant structure factors for different models of symmetric binary blends with soft repulsive potential. Each panel contains plots for models having similar $\bar{N}$; points of different colors correspond to different models. Each model was simulated at $\chi_e N = 0$ and $\chi_e N = 2$. Dashed curves show the random phase approximation (RPA) predictions.

at $n = 4$ approximates the series well for all α used in this work (Sec. 5 in the Supplemental Material [24]); the apparent convergence of Eq. (9) for all studied models agreed with the theoretical prediction of convergence radius of Eq. (9), which was predicted to be $\approx a_{xx}$, which is much greater than α values used in all models in this work. We will use Eq. (9) truncated at $n = 4$ to estimate χ_e for all models simulated in this work. Table S1 in the Supplemental Material [24]contains the values of $\bar{N}$, b, and $\kappa_n[z]_{0,N\to\infty}$ for all studied models.

IV. SIMULATION RESULTS

First, we constructed 11 different models of symmetric binary blends with soft repulsive potential; they formed four groups having similar $\bar{N}$ spanning the experimentally relevant [7] range of $\bar{N} \in [10^2, 10^4]$. Within each group, the values of $\bar{N}$ differed by no more than 4%. Model parameters can be found in Fig. 1. We performed simulations in NVT ensemble and equilibrated the models at $\chi_e N \in [0, 5]$. The influence of the finite simulation box size on the universality of blend models was removed via the simulation box size rescaling technique; see Sec. 3 in the Supplemental Material [24] for simulation details. At each value of $\chi_e N$, we measured the excess free energy per chain F using the Bennett acceptance ratio method [29] and the invariant structure factor $S(q)/\rho N$, where $S(q)$ is the Fourier transform of the composition fluctuations correlation function [16].

Figures 1 and 2 show that defining $\chi_e(\alpha)$ according to Eq. (9) led to the universal behavior of the studied models. First, F (and its derivative with respect to $\chi_e N$, Fig. S5 in the Supplemental Material [24]) depended only on the $\chi_e N$ parameter at each value of $\bar{N}$ below and above the phase separation point $\chi_e N \approx 2$; other model parameters affected F negligibly. Second, the value of $S(q)/\rho N$ at large length scales (for $qR_g^0 \lesssim 2.5$ and except the poor-statistics region $qR_g^0 \approx 0.5$) depended almost exclusively on $\bar{N}$, $\chi_e N$, and the normalized wave number qR_g^0, where $R_g^0 = b(N/6)^{1/2}$ is the characteristic chain radius of gyration (Fig. 2). For bigger wave numbers, the microscopic structure of models started to influence the $S(q)/\rho N$ functions leading to their divergence.

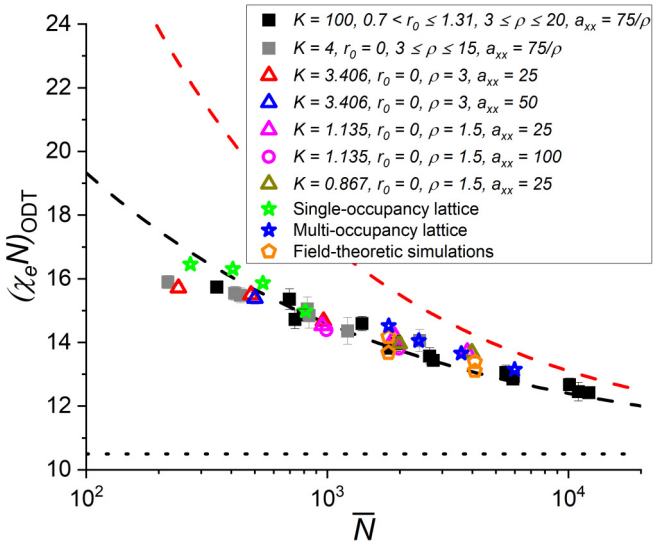


FIG. 3. $\bar{N}$ dependency of $\chi_e N$ at the order-disorder transition point $[(\chi_e N)_{\mathrm{ODT}}]$ for symmetric diblock copolymer melt models. The data for field-theoretic simulations, single- and multioccupancy lattice models are taken from Refs. [31,32], [7], and [21], respectively. The values of $\alpha_{\mathrm{ODT}}/k_B T$ for MD models with soft repulsive potential were obtained in Ref. [16]; Table S1 in the Supplemental Material [24] contains more detailed parameters. The predictions of RPA [33], Fredrickson-Helfand (FH) theory [9], and Morse *et al.* universal fit [7] are shown as black dotted line, black dashed curve, and red dashed curve, respectively.

This behavior agreed well with the universality hypothesis [7,16] and supported the soundness of our perturbative definition of χ_e for binary blend models.

To confirm that this definition is applicable to the systems with other chain architectures, we studied the models of symmetric DBC melts. Figure 3 shows the dependency of $\chi_e N$ at the order-disorder transition on $\bar{N}$ for MD models with soft repulsive potential, the single and multioccupancy lattice models, and field-theoretic simulations. We obtained the values of $\alpha_{\mathrm{ODT}}/k_B T$ (or $(\chi_b)_{\mathrm{ODT}}$ for FTS) to calculate $(\chi_e N)_{\mathrm{ODT}}$ from Refs. [7,16,21,31,32]. For FTS and lattice models, only z_∞ values were published without other moments of the z distributions. In Sec. 4 in the Supplemental Material [24], we evaluated how $O(\alpha^2)$ terms affect $(\chi_e N)_{\mathrm{ODT}}$ for these models; if this effect was $\lesssim 1\%$ (which corresponded to the shift within the symbol size), we included data for FTS and lattice models in Fig. 3 using the $\chi_e = z_\infty \chi_b$ and $\chi_e = z_\infty \alpha/k_B T$ expressions, respectively. For MD models with soft repulsive potential, we calculated $\kappa_n[z]_{0,N\to\infty}$ up to $n = 4$ to calculate $\chi_e(\alpha)$ using Eq. (9) as mentioned before.

In accord with the universality hypothesis, $(\chi_e N)_{\mathrm{ODT}}$ values depended almost solely on $\bar{N}$ and formed a master curve (data for models with soft repulsive potential deviated from each other by no more than 4% at a similar $\bar{N}$ as in Ref. [7]). Interestingly, the data agreed well with the curve predicted by the classical FH theory, which, however, is strictly valid at much higher $\bar{N}$ [9]. Moreover, $(\chi_e N)_{\mathrm{ODT}}$ values deviated significantly from the ROL theory-based universal curve [7], which potentially points at poorer applicability of this theory near the ODT point. In addition, $(\chi_e N)_{\mathrm{ODT}}$ values started to slightly deviate from the FH-like master curve at low enough $\bar{N} \lesssim 400$, which is similar to the behavior of DBC models at $\bar{N} \approx 100$ in Ref. [7]. Therefore, $\bar{N} \approx 100$ is the possible lower bound for the validity of the universality hypothesis.

To further investigate the behavior of DBC models, we performed MD simulations of nine symmetric DBC melt models organized into three groups with similar $\bar{N}$ values ($\bar{N} \approx 300$, $\bar{N} \approx 800$, and $\bar{N} \approx 4000$, $\bar{N}$ in each group varied by no more than 5%). The parameters of models are listed in Fig. 4; Sec. 3 in the Supplemental Material [24]contains the simulation details. We equilibrated the systems at $\chi_e N \in [0, 20]$ and studied the dependencies of the excess free energy per chain F and its $\chi_e N$ derivative on $\chi_e N$. For the models with $\bar{N} \approx 800$ and $\bar{N} \approx 4000$, these dependencies agreed well with each other as predicted by the universality hypothesis [Figs. 4(b), 4(c), 4(e), 4(f)]. At small $\bar{N} \approx 300$, a moderate nonuniversal discrepancy of F and its derivative was observed between the models at high $\chi_e N$ [Figs. 4(a) and 4(d)]. These data confirmed that the perturbative definition of χ_e [Eq. (9)] starts to become somewhat nonuniversal for $\bar{N} \lesssim 400$.

Finally, we analyzed the invariant structure factors for the simulated models. Their mesoscopic behavior can be characterized by the normalized peak wave number $(q^* R_g^0)$ and the peak scattering intensity $S(q^*)/\rho N$. These values can be determined [16,22] by fitting the invariant structure factor with a smooth function in the range $qR_g^0 \in [1, 3]$. Figure 5 showed that these quantities depended only on $\chi_e N$ and $\bar{N}$ within the uncertainty of estimation for all studied models with any $\bar{N}$, confirming the universality hypothesis. Interestingly, the free energy appears to be more sensitive to the onset of nonuniversal behavior of models than their mesoscopic structure, which can still remain universal below $\bar{N} \approx 300$ [Figs. 5(a) and 5(d)].

As described in Sec. II, we developed a separate theory to understand in detail how model parameters influence χ_e. In particular, we determined what controls the cumulants $\kappa_n[z]_{0,N\to\infty}$ in Eq. (9). We found that $\kappa_n[z]_{0,N\to\infty}$ are mostly determined by the quantity ρ/a_{xx}^n in continuum particle-based models at a fixed T [Eq. (10)]. This was qualitatively confirmed in our simulations (Fig. S4 in the Supplemental Material [24]). From this, we derived that the minimal order of truncation of Eq. (9) depends mostly on the value of $N\rho$ at a given $\chi_e N$ and truncation tolerance and changes weakly with other model parameters. Figure. 6(a) confirmed this picture qualitatively. In particular, two different models with the same N and ρ had similar discrepancy between $\chi_e N$ in the linear ($\chi_e \propto \alpha$) and nonlinear [Eq. (9) truncated at $n = 4$] approximations at any fixed $\chi_e N$ value. As a result, Eq. (9) had to be truncated at the same ($n = 3$) order for both of these models to determine χ_e accurately for $\chi_e N \leqslant 20$. On the other hand, an increase of either N or ρ led to a much smaller discrepancy between the two estimations of $\chi_e N$. This shows that χ_e can be accurately determined according to the linear $\chi_e \propto \alpha$ approximation for models with high enough $N\rho$.

We determined this threshold value of $N\rho$ for $\alpha = \alpha_{\mathrm{ODT}}$ theoretically and based on the simulation data on continuum particle-based models in Fig. 6(b). Using Eq. (10), we obtained that the ratio of the second- and first-order terms in Eq. (9) (which characterizes how strongly the nonlinear

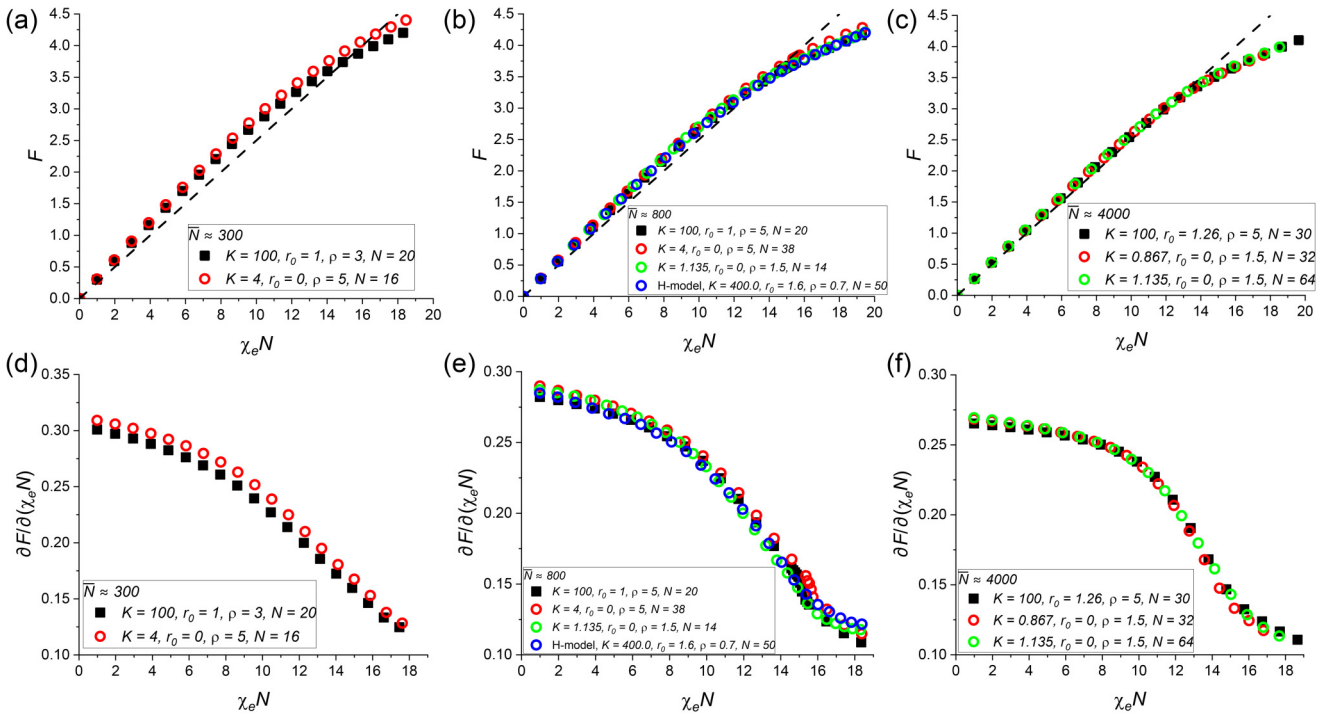


FIG. 4. $\chi_e N$dependencies of the excess free energy per chain F [panels (a)–(c)] and their $\chi_e N$-derivatives [panels (d)–(f)] for different MD models of symmetric diblock copolymer melts (except for H model, all models had soft repulsive potential). Each panel contains plots for models having similar $\bar{N}$; points of different colors correspond to different models. Except for models with $\rho = 1.5$, a_{xx} was calculated as $a_{xx} = 75/\rho$, models with $\rho = 1.5$ had $a_{xx} = 25$. H model had $a_{xx} = 1.0$. Dashed lines show the mean-field prediction $F = \chi_e N/4$.

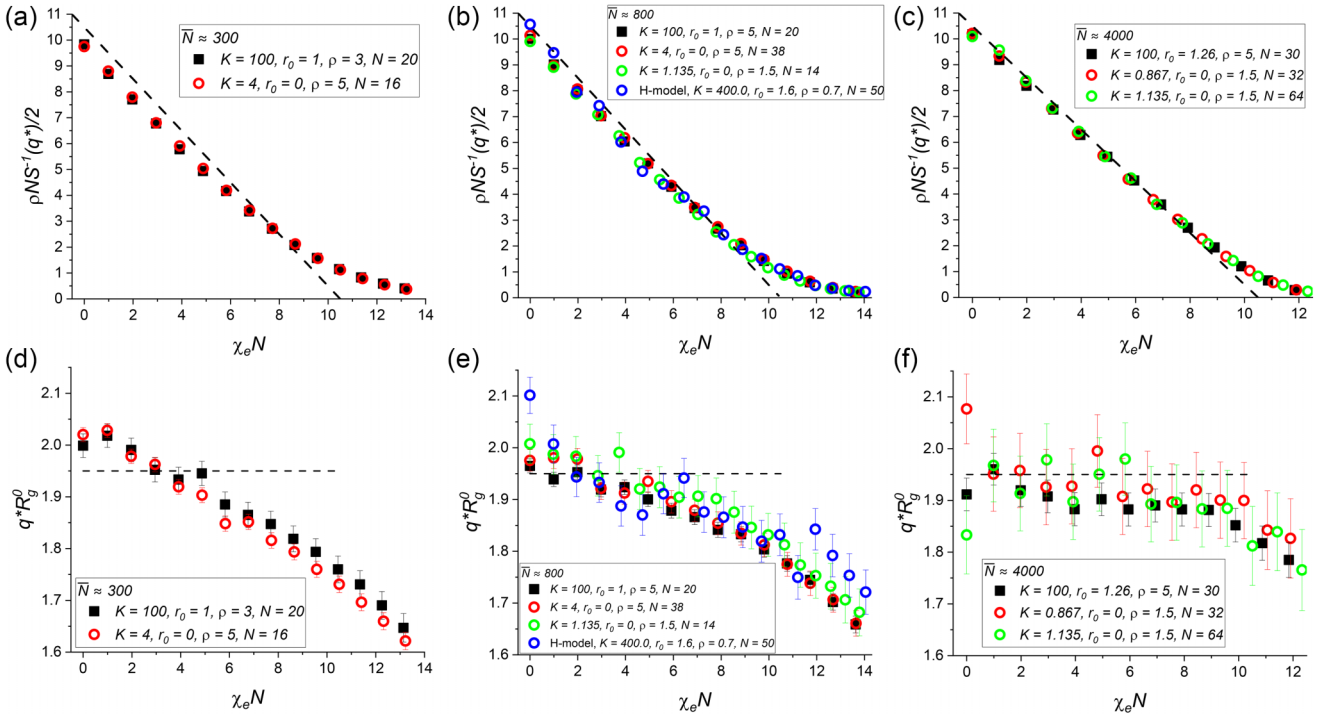


FIG. 5. $\chi_e N$ dependencies of the inverse peak scattering intensity [panels (a)–(c)] and the normalized peak wave number [panels (d)–(f)] for different MD models of symmetric diblock copolymer melts (except for H model, all models had soft repulsive potential). Each panel contains plots for models having similar $\bar{N}$; points of different colors correspond to different models. Dashed lines show RPA predictions.

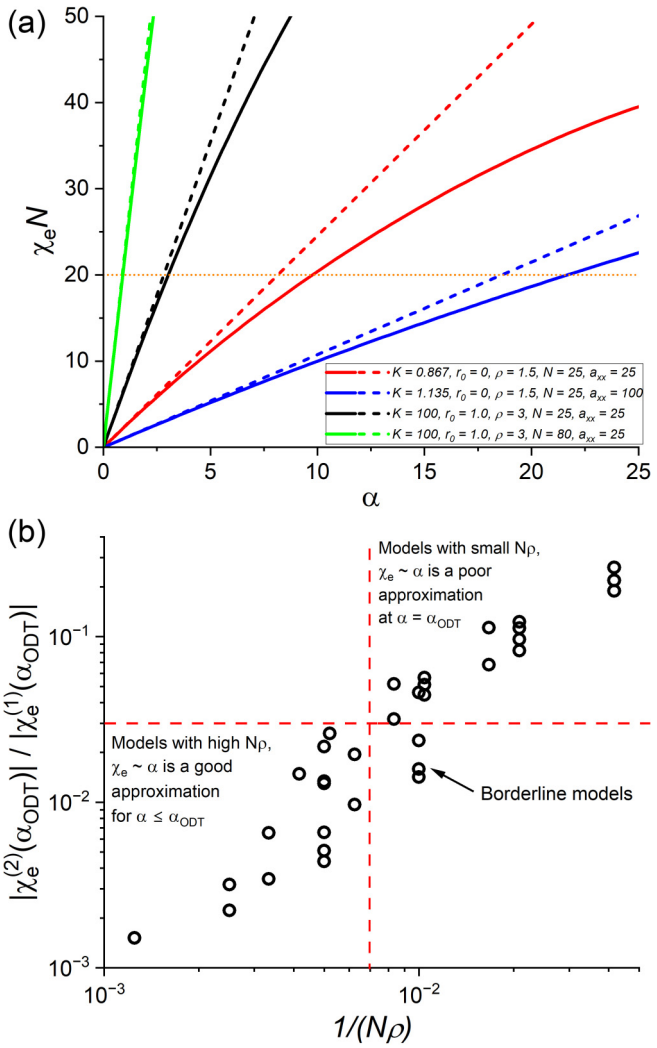


FIG. 6. (a) Dependence of $\chi_e(\alpha)N$ at fixed $k_BT = 1$ for some of the studied models. Solid and dashed curves correspond to Eq. (9) truncated at $n = 4$ (used in Figs. 1–5 for all models simulated in MD) and at $n = 1$, respectively. The values of $\kappa_n[z]_{0,N\to\infty}$ parametrizing Eq. (9) for each model are listed in Table S1 in the Supplemental Material [24]. The horizontal dotted line shows the maximal $\chi_e N = 20$ value used in this work. (b) The dependency of the ratio of the second term in Eq. (9) to the first (linear) term at $\alpha = \alpha_{ODT}$ on $1/N\rho$ in the studied models of symmetric diblock copolymer melts. The horizontal red line shows the approximate boundary of the $\chi_e \propto \alpha$ approximation applicability for $\alpha \leqslant \alpha_{ODT}$, and the vertical line shows the corresponding threshold value $1/(N\rho)_c$.

corrections affect the value of χ_e for a given model) depends solely on $1/N\rho$ at $\alpha = \alpha_{ODT}$. The existence of a master curve in Fig. 6(b) supports this prediction qualitatively. Crucially, when $N\rho$ surpassed a certain characteristic value $(N\rho)_c$, this ratio became lower than some small threshold (0.03 in this work). In turn, this means that the linear approximation $\chi_e = z_\infty \alpha/k_BT$ worked well for the models with high enough $N\rho$ at or below ODT. This theoretically explains the existence of finite-N, high-ρ models of symmetric diblock copolymers that behave universally in the $\chi_e \propto \alpha$ approximation as discovered in Ref. [16] (see Fig. S6 for additional data). Equation (10) predicts $(N\rho)_c \approx 60$ (Sec. 8 in the Supplemental Material [24]), which agrees well by an order of magnitude with the $(N\rho)_c \approx 140$ value established empirically in Fig. 6(b).

V. DISCUSSION AND CONCLUSIONS

In conclusion, we developed an approximate perturbation theory for binary polymer blends and derived an analytical expression for the effective Flory-Huggins parameter χ_e as a series in powers of α: the energy parameter characterizing the imbalance between opposite- and same-type interactions in a coarse-grained model [Eq. (9)]. This formula has a clear physical meaning and can be parametrized much more easily than the previous definition [7] by measuring the cumulants of the distribution of the effective monomer coordination number in a reference homogeneous system. Moreover, a direct qualitative link between these cumulants and the model parameters can be established, which clarifies the microscopic nature of χ_e and elucidates how the construction of a model can influence χ_e (including its polynomial degree). By performing extensive MD simulations and using available data on the lattice models and FTS, we showed that our perturbative definition of χ_e is able to yield the universal behavior of coarse-grained models of different two-component symmetric polymer systems in the experimentally relevant range $\bar{N} \gtrsim 400$ and for $\chi_e N$ at least as high as $\chi_e N \approx 20$, which supported the soundness of the χ_e expression (for our definition of a model; see Sec. 6 in the Supplemental Material [24]). Moreover, we provided additional support for the universality hypothesis without assuming *a priori* the universality of any of the model characteristics. As a result, our definition of χ_e can be used to easily and quantitatively map different coarse-grained models of multicomponent polymer systems onto each other and to quantitatively compare coarse-grained simulations to experiments. We expect our results to hold for asymmetric and multicomponent polymers as well, since the fitting-based χ_e defined for symmetric DBC systems could yield the universality of asymmetric DBC melts [27,28]; this is left for future research.

Two interesting features uncovered in this work are worth noting here. First, the universality of models based on Eq. (9) can be explained by a presumed good agreement of the dominant low-order terms in Eq. (9) with those predicted by a "true" perturbation theory that takes all correlations into account (see Sec. 7 in the Supplemental Material [24] for justification). In turn, this hypothetical "exact" perturbation theory should give correct Δf_{int} in a disordered system in some finite α/k_BT range, since all nonbonded interaction potentials used in this work are stable and tempered [34]. As a result, Eq. (9) could yield a nearly correct expression for χ_e in that range as well. Presumably, at higher α, χ_e continues to be mostly determined by the fluctuations of z as for small α; these fluctuations, in turn, depend on α weakly. This can explain the observed universality at and beyond the phase transition points in this work (Figs. 1, 3, and 4) and in Ref. [7], where the coefficients for the $\chi_e(\alpha)$ function were also determined in a nonseparated state. However, the rigorous clarification of this phenomenon is a good topic for future research. Second, the analytical expression for $\chi_e(\alpha)$ that we derived here had a limited success in yielding universality for another definition of a

"model" considered in Refs. [7,8], where the system *pressure*, and not the density ρ, was fixed with α. This shortcoming may stem from the approximate nature of the perturbation theory developed here and can be overcome by calculating $\chi_e(\alpha)$ in an equivalent (at a certain α in thermodynamic limit) NVT model having $\rho = \bar{\rho}(\alpha)$, where $\bar{\rho}(\alpha)$ is the average density at the given α in the studied model with fixed pressure (Sec. 6 in the Supplemental Material [24]).

ACKNOWLEDGMENTS

We thank C. Marty and T. Jin for their help and fruitful discussions. We also thank D. Morse for insightful comments. We acknowledge the MIT SuperCloud and Lincoln Laboratory Supercomputing Center as well as the MIT Office of Research Computing and Data for providing high-performance computing resources. This research was supported by the National Science Foundation through Award No. DMREF 2118678.

DATA AVAILABILITY

The data that support the findings of this article are not publicly available upon publication because it is not technically feasible and/or the cost of preparing, depositing, and hosting the data would be prohibitive within the terms of this research project. The data are available from the authors upon reasonable request.

[1] C. Koning, M. Van Duin, C. Pagnoulle, and R. Jerome, Strategies for compatibilization of polymer blends, Prog. Polym. Sci. **23**, 707 (1998).

[2] C. Sinturel, F. S. Bates, and M. A. Hillmyer, High χ–low n block polymers: How far can we go? ACS Macro Lett. **4**, 1044 (2015).

[3] K. D. Dorfman, Computational phase discovery in block polymers, ACS Macro Lett. **13**, 1612 (2024).

[4] D. S. Marques, U. Vainio, N. M. Chaparro, V. M. Calo, A. R. Bezahd, J. W. Pitera, K.-V. Peinemann, and S. P. Nunes, Self-assembly in casting solutions of block copolymer membranes, Soft Matter **9**, 5557 (2013).

[5] W. Gu, J. Huh, S. W. Hong, B. R. Sveinbjornsson, C. Park, R. H. Grubbs, and T. P. Russell, Self-assembly of symmetric brush diblock copolymers, ACS Nano **7**, 2551 (2013).

[6] A. V. Berezkin, F. Jung, D. Posselt, D. M. Smilgies, and C. M. Papadakis, Vertical vs lateral macrophase separation in thin films of block copolymer mixtures: Computer simulations and GISAXS experiments, ACS Appl. Mater. Interfaces **9**, 31291 (2017).

[7] J. Glaser, P. Medapuram, T. M. Beardsley, M. W. Matsen, and D. C. Morse, Universality of block copolymer melts, Phys. Rev. Lett. **113**, 068302 (2014).

[8] P. Medapuram, J. Glaser, and D. C. Morse, Universal phenomenology of symmetric diblock copolymers near the order–disorder transition, Macromolecules **48**, 819 (2015).

[9] G. H. Fredrickson and E. Helfand, Fluctuation effects in the theory of microphase separation in block copolymers, J. Chem. Phys. **87**, 697 (1987).

[10] P. Grzywacz, J. Qin, and D. C. Morse, Renormalization of the one-loop theory of fluctuations in polymer blends and diblock copolymer melts, Phys. Rev. E **76**, 061802 (2007).

[11] J. Qin and D. C. Morse, Renormalized one-loop theory of correlations in polymer blends, J. Chem. Phys. **130**, 224902 (2009).

[12] J. Qin, P. Grzywacz, and D. C. Morse, Renormalized one-loop theory of correlations in disordered diblock copolymers, J. Chem. Phys. **135**, 084902 (2011).

[13] D. C. Morse and J. K. Chung, On the chain length dependence of local correlations in polymer melts and a perturbation theory of symmetric polymer blends, J. Chem. Phys. **130**, 224901 (2009).

[14] T. M. Gillard, P. Medapuram, D. C. Morse, and F. S. Bates, Fluctuations, phase transitions, and latent heat in short diblock copolymers: Comparison of experiment, simulation, and theory, Macromolecules **48**, 2801 (2015).

[15] T. M. Beardsley and M. W. Matsen, Universality between experiment and simulation of a diblock copolymer melt, Phys. Rev. Lett. **117**, 217801 (2016).

[16] A. Petrov, H. Huang, and A. Alexander-Katz, Simple calibration of block copolymer melt models, Macromolecules **57**, 8212 (2024).

[17] F. S. Bates, J. H. Rosedale, and G. H. Fredrickson, Fluctuation effects in a symmetric diblock copolymer near the order–disorder transition, J. Chem. Phys. **92**, 6255 (1990).

[18] J. K. Chung, *Correlations in Polymer Blends: Simulations, Perturbation Theory, and Coarse-Grained Theory* (University of Minnesota, Ann Arbor, MA, 2009).

[19] A. Petrov, A. V. Chertovich, and A. A. Gavrilov, Phase diagrams of polymerization-induced self-assembly are largely determined by polymer recombination, Polymers **14**, 5331 (2022).

[20] A. Petrov, P. Kos, and A. Chertovich, Kinetic mechanisms of crumpled globule formation, Soft Matter **16**, 2045 (2020).

[21] J. Willis, T. Beardsley, and M. Matsen, Calibration of a lattice model for high-molecular-weight block copolymer melts, J. Chem. Phys. **150**, 204906 (2019).

[22] J. Glaser, J. Qin, P. Medapuram, and D. C. Morse, Collective and single-chain correlations in disordered melts of symmetric diblock copolymers: Quantitative comparison of simulations and theory, Macromolecules **47**, 851 (2014).

[23] M. W. Matsen, T. M. Beardsley, and J. D. Willis, Fluctuation-corrected phase diagrams for diblock copolymer melts, Phys. Rev. Lett. **130**, 248101 (2023).

[24] See Supplemental Material at http://link.aps.org/supplemental/10.1103/532b-lhkh for detailed derivations, expressions for $n \to \infty$ extrapolation of the relevant quantities, detailed simulation protocols, and data supporting claims in the main text, which also includes Refs. [35–37].

[25] C. Chipot and A. Pohorille, *Free Energy Calculations* (Springer, Berlin, Germany, 2007), Vol. 86.

[26] D. R. Brillinger, Moments, cumulants and some applications to stationary random processes, Technical Report No. **459** 108, 1992.

[27] T. Ghasimakbari and D. C. Morse, Correlations in disordered melts of asymmetric diblock copolymers, Macromolecules **51**, 2335 (2018).

[28] T. Ghasimakbari and D. C. Morse, Order-disorder transitions and free energies in asymmetric diblock copolymers, Macromolecules **53**, 7399 (2020).

[29] C. H. Bennett, Efficient estimation of free energy differences from Monte Carlo data, J. Comput. Phys. **22**, 245 (1976).

[30] R. D. Groot and P. B. Warren, Dissipative particle dynamics: Bridging the gap between atomistic and mesoscopic simulation, J. Chem. Phys. **107**, 4423 (1997).

[31] T. Beardsley, R. Spencer, and M. Matsen, Computationally efficient field-theoretic simulations for block copolymer melts, Macromolecules **52**, 8840 (2019).

[32] T. Beardsley and M. Matsen, Calibration of the Flory-Huggins interaction parameter in field-theoretic simulations, J. Chem. Phys. **150**, 174902 (2019).

[33] L. Leibler, Theory of microphase separation in block copolymers, Macromolecules **13**, 1602 (1980).

[34] J. Lebowitz and O. Penrose, Convergence of virial expansions, J. Math. Phys. **5**, 841 (1964).

[35] P.-G. De Gennes, *Scaling Concepts in Polymer Physics* (Cornell University Press, Ithaca, NY, 1979).

[36] M. P. Allen and D. J. Tildesley, *Computer Simulation of Liquids* (Oxford University Press, Oxford, UK, 2017).

[37] E. Helfand and Y. Tagami, Theory of the interface between immiscible polymers, J. Polym. Sci. Part B: Polym. Phys. **9**, 741 (1971).